30. Buffer A consists of 10 mM tris-acetate (pH 7.5 at 4°C), 40 mM β-glycerophosphate, 1.5 mM EGTA, 0.5 mM EDTA, 25 mM sodium fluoride, 1 mM sodium pyrophosphate, 0.5 mM sodium orthovanadate, 1 mM dithiothreitol, 1 mM benzamidine, 0.5% (v/v) Triton X-100, phenylmethylsulfonylfluoride (0.1 mg/ml), 1 μM pepstatin A, leupeptin (2 μg/ml), and aprotinin (2 μg/ml).
31. B. Margolis *et al.*, *Mol. Cell. Biol.* **10**, 435 (1990).
32. A. J. Rossomando, D. M. Payne, M. J. Weber, T. W. Sturgill, *Proc. Natl. Acad. Sci. U.S.A.* **86**, 6940 (1989).
33. For the in vivo studies, cells were quickly chilled and washed twice with ice-cold phosphate-buffered saline, sedimented, and resuspended in p21 buffer (*3*) (100 μl per 15-cm plate). In later experiments, additional phosphatase inhibitors (10 mM Na_2VO_4, 10 mM *p*-nitrophenyl phosphate, 40 mM β-glycerol phosphate, 25 mM NaF, 1 μM microcystin-LR, 0.01 μM calyculin A, and 0.2 mM sodium pyrophosphate) were included in all buffers and appear to be important for preserving the effect of forskolin on Raf-1. Resuspended cells were homogenized (*27*), and the lysates were centrifuged (100,000*g* at 4°C for 30 min). Approximately 40 μg of supernatant protein was incubated (200 μl total volume at 4°C for 30 min) with 50 μg of immobilized c-Ha-Ras, loaded with GMP-PNP or GDP (*3*). Beads were sedimented by brief centrifugation (15,000*g* for 1 min), and supernatants were removed. Beads were resuspended in 200 μl of p21 buffer containing CHAPS (0.1% w/v) and layered onto 5× p21 buffer (1 ml in a 1.5-ml tube) and centrifuged. Recovered beads were washed (4× with 1 ml of p21 buffer with CHAPS). Adsorbed proteins were released with SDS sample buffer and processed by SDS-PAGE (on 8% gels) for protein immunoblotting with antibodies to Raf-CR2 (conserved region 2) (anti–Raf-CR2); immunoblots were developed by enhanced chemiluminescence. Raf band intensities of immunoblots were quantitated on the basis of the local background by a densitometer (Molecular Dynamics, Sunnyvale, CA).
34. Supported by grants from NIH to T.W.S. (DK41077) and to M.J.W. (CA39076) and from the American Cancer Society to T.W.S. (BE69D) and by Young Investigator Awards to P.D. and J.W. from the Virginia affiliate of the American Diabetes Association. Fellowship support for J.W. came from the Juvenile Diabetes Foundation International. We especially thank D. Morrison (ABL-Basic Research Program, Frederick, MD) for providing recombinant Raf(K375M) baculovirus, the anti–Raf-CR2, synthetic Raf-1 peptides, and many helpful discussions. We also thank L. A. Vincent for technical assistance; J. Schlessinger (New York University) and R. Schatzman (Syntex, Palo Alto, CA) for antibodies to the EGFR and Raf–COOH-terminus, respectively; and J. Corbin (Vanderbilt University) for PKA.

17 August 1993; accepted 5 October 1993

Inhibition by cAMP of Ras-Dependent Activation of Raf

Simon J. Cook* and Frank McCormick

Activation of the Raf and extracellular signal–regulated kinases (ERKs) (or mitogen-activated protein kinases) are key events in mitogenic signaling, but little is known about interactions with other signaling pathways. Agents that raise levels of intracellular cyclic adenosine 3′,5′-monophosphate (cAMP) blocked DNA synthesis and signal transduction in Rat1 cells exposed to epidermal growth factor (EGF) or lysophosphatidic acid. In the case of EGF, receptor tyrosine kinase activity and association with the signaling molecules Grb2 and Shc were unaffected by cAMP. Likewise, EGF-dependent accumulation of the guanosine 5′-triphosphate–bound form of Ras was unaffected. In contrast, activation of Raf-1 and ERK kinases was inhibited. Thus, cAMP appears to inhibit signal transmission from Ras by preventing Ras-dependent activation of Raf-1.

Cyclic adenosine 3′,5′-monophosphate (cAMP) was the first second messenger to be identified, and its role in regulating physiological processes is well established (*1*). Hormone receptors increase the intracellular concentration of cAMP by increasing the amount of the free α subunit of the guanosine triphosphate (GTP) binding protein G_s ($G\alpha_s$·GTP), which activates adenylyl cyclase (*2, 3*). Despite literature dating back 25 years (*3*), the precise role of cAMP in regulating cell growth and proliferation remains a matter of considerable debate (*3, 4*). In some cells, such as Swiss 3T3 cells and thyrocytes, cAMP is a mitogenic messenger and promotes the G_1 to S phase transition in the cell cycle (*4*). In contrast, cAMP inhibits the proliferation of many cell lines, including fibroblasts, T cells, neuroblastoma and astrocytoma cells, and cells transformed by Ras, Src, and polyoma middle T antigen (*3*).

Kinetic analysis indicates cAMP exerts a cytostatic effect in the early G_0 to G_1 phase as well as mid-G_1 phase (*5*) and, in a few cases, G_2 (*3*). Cyclic AMP inhibits proliferation by growth factors irrespective of their ability to activate the polyphosphoinositide (PI) pathway; therefore, the ability of cAMP to inhibit full activation of the PI pathway is unlikely to explain its effects (*5*). Because cAMP inhibits proliferation stimulated by receptor tyrosine kinases or GTP binding protein–coupled or "serpentine" receptors, it is more likely to exert its effect downstream of receptor activation and second messenger generation, where signal transduction pathways converge.

Onyx Pharmaceuticals, 3031 Research Drive, Richmond, CA 94806.

*To whom correspondence should be addressed.

A common point of convergence for many, if not all, growth factors is the activation of the Ras proteins (*6*), which regulate signals to the mitogen-activated protein kinases ERK1 and ERK2 (*7*). These are serine-threonine kinases that require phosphorylation at both tyrosine and threonine for activation; both phosphorylation events are catalyzed by the same dual-specificity mitogen-activated protein (MAP) kinase kinase called MAP or ERK kinase (MEK) (*8*). MEK is in turn regulated by at least two upstream kinases: the c-Raf-1 proto-oncogene product (*9*) or MEK kinase (*10*). The stimulation of quiescent cells with various growth factors or phorbol esters or the introduction of oncogenic Ras proteins leads to the activation of ERKs within minutes (*7*). Indeed, Ras is required for growth factors to fully activate the Raf-MEK-ERK pathway (*7, 11*), which suggests that Ras is a common target for growth factors and that this kinase cascade is important for regulating the G_1 to S phase transition. In Rat1 cells, Ras is a point of convergence for two different classes of growth factor, lysophosphatidic acid (LPA) or epidermal growth factor (EGF), to fully stimulate DNA synthesis and ERK activation (*11*). Here, we have examined the effect of cAMP on growth factor stimulation of ERK1 and ERK2.

Quiescent Rat1 cells were incubated with 1 mM dibutyryl cAMP for 10 min before stimulation with LPA or EGF, and ERK activation was assayed on protein immunoblots by the appearance of activated, hyperphosphorylated forms with retarded mobility on SDS–polyacrylamide gel electrophoresis (SDS-PAGE). Dibutyryl cAMP alone had no effect on the activation of ERK1 and ERK2 in Rat1 cells, but a 10-min treatment with dibutyryl cAMP completely inhibited the LPA- or EGF-induced mobility shift (Fig. 1A); 8-bromo–cAMP was also effective (*12*). With a more sensitive immune complex kinase assay (*13*), we found that the ability of the phorbol ester PMA (phorbol 12-myristate 13-acetate) to activate MAP kinases, albeit a submaximal activation compared with that of EGF, was also inhibited by dibutyryl cAMP (Fig. 1B). These effects were not due to contamination of dibutyryl cAMP with butyrate or metabolic release of butyrate within the cell because butyrate itself (up to 1 mM) did not inhibit ERK1 (Fig. 1B) or DNA synthesis (*12*). Furthermore, a 10-min exposure to dibutyryl cAMP did not affect the amount of immunoreactive ERK1 and ERK2 (Fig. 1A), so the loss of ERK activity (Fig. 1B) did not result from a decreased amount of the enzyme. The 50% inhibition concentration (IC_{50}) of dibutyryl cAMP upon LPA- or EGF-stimulated ERK1 was approximately 0.1 to 0.2 mM, which agreed with that for inhibition of DNA synthesis (*12*).

The adenosine diphosphate (ADP) ribo-

syl transferase activity of cholera toxin (CT) specifically adds an ADP ribose group to $G\alpha_s$, which results in inhibition of the intrinsic guanosine triphosphatase (GTPase) activity of $G\alpha_s$·GTP and constitutive activation of adenylyl cyclase (*14*). Treatment of Rat1 cells with increasing concentrations of CT resulted in a dose-dependent inhibition of subsequent ERK1 activation by EGF measured by the ability of the immunoprecipitated ERK1 to phosphorylate myelin basic protein (MBP) (Fig. 2A). The IC_{50} for the effect of CT (0.17 ± 0.15 ng/ml) fell within the range of the IC_{50} for CT-mediated inhibition of DNA synthesis by EGF (0.03 ± 0.01 ng/ml) (Fig. 2B). The effect of submaximal doses of CT on EGF-stimulated ERK activation was greatly potentiated by the cAMP phosphodiesterase inhibitor 3-isobutyl-1-methylxanthine (IBMX) (50 μM), which resulted in a shift of the CT dose-response curve to the left by one to one and a half orders of magnitude (Fig. 2A). This potentiation of low doses of CT by IBMX was also noted for its inhibition of EGF- or LPA-stimulated DNA synthesis (*12*) and represents the ability of IBMX to block metabolic conversion of cAMP, thereby resulting in more persistent and increased concentrations of cAMP even with small amounts of CT (*15*). The fact that both ERK activation and DNA synthesis were inhibited by both cAMP analogs and CT, together with the observed synergy between IBMX and small doses of CT, strongly suggests that CT exerts its effects through elevation of cAMP in this system.

The major elements required for functional coupling of the EGF receptor (EGFR) to ERKs have been identified (*16*). The Src homology 2 (SH2)–SH3 adaptor protein Grb2 recruits the Ras exchange factor Sos to the activated EGFR at the plasma membrane where it activates Ras (*16*). We studied the effect of cAMP on EGFR phosphorylation and signaling complex assembly by assaying the binding of the activated EGFR to the glutathione-S-transferase–Grb2 fusion protein (GST-Grb2) in vitro (*17*). Cell lysates from control or EGF-treated Rat1 cells previously incubated with or without CT were incubated with GST-Grb2. Bound proteins were detected by protein immunoblotting with monoclonal antibodies to phosphotyrosine (PY20 and PY69; ICN, Irvine, California).

Phosphotyrosine-containing proteins were not detectable in GST precipitates from either control or EGF-stimulated cells (*12*, *18*). In GST-Grb2 precipitates, we observed the association of several phosphotyrosine-containing proteins with GST-Grb2 in an EGF-dependent manner, including a broad, heavily phosphorylated band at approximately 170 to 180 kD. This protein appears to be the autophosphorylated EGFR because it comigrated with the human EGFR in similar experiments done in HER14 cells (*12*). We also observed other tyrosine phosphoproteins (p52, p55, p66, and p116) that coprecipitated with the EGFR in an EGF-dependent manner. Protein immunoblotting of the same samples resolved on the same gel with a polyclonal antibody to Shc confirmed the identity of two of these proteins as $p52^{shc}$ and $p66^{shc}$. Shc is an SH2 domain–containing protein that is implicated in the coupling of receptor and nonreceptor tyrosine kinases to Ras and that can transform cells when overexpressed (*19*). Thus, EGF stimulation results in the assembly of multimeric signaling complexes at the EGFR that include Grb2, Shc, and other phosphoproteins. In cells pretreated with CT, we observed no inhibition of EGFR autophosphorylation or association of EGFR signaling complexes with GST-Grb2 (Fig. 3A).

EGF activation of ERK1 and ERK2 proceeds through a Ras-dependent pathway (*7*, *11*), and EGF treatment of Rat1 cells for 5 min resulted in an increase in the percentage of Ras in the GTP-bound form from 12 to 30 to 35%. Treatment of Rat1 cells with 1 mM dibutyryl cAMP for 10 min had no effect on the ability of EGF to increase the amount of Ras·GTP in Rat1 cells (Fig. 3B). Thus, under conditions in which EGFR phosphorylation, EGFR signaling complexes, and EGFR signaling to Ras were all intact, the ability of EGF to activate ERK1 and ERK2 was completely inhibited.

Raf-1 has been defined genetically and biochemically as being a likely target of Ras (*20*), and Ras is critical for activation of

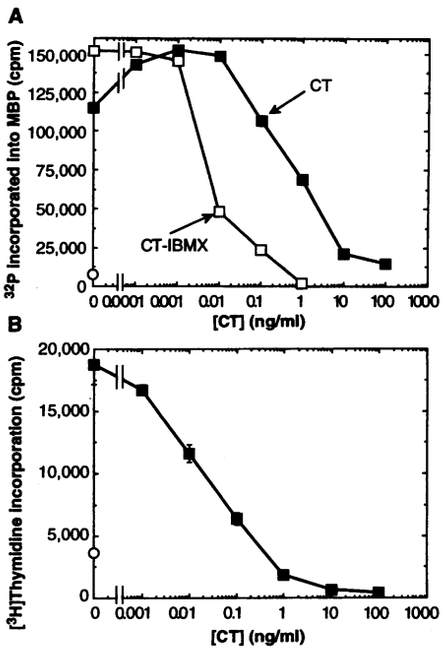

Fig. 2. Effects of CT on EGF-stimulated ERK1 activity and DNA synthesis in Rat1 cells. (**A**) Inhibition by CT of EGF-stimulated ERK1 activation in Rat1 cells. Quiescent cells were incubated for 1 hour with various concentrations of CT alone (■) or in the presence of IBMX (50 μM) (□) before stimulation with 10 nM EGF for 5 min. After lysis, ERK1 immunoprecipitates were assayed for MBP kinase activity. Results are expressed as the amount of ^{32}P incorporated into MBP (counts per minute) and are from a single experiment representative of three that gave similar results. (**B**) Inhibition of EGF-stimulated DNA synthesis in Rat1 cells by CT. Quiescent cells were stimulated with 10 nM EGF in the presence of increasing concentrations of CT. [^{3}H]Thymidine (3 μM unlabeled thymidine) was added for the last 2 hours, and the reactions were terminated after 22 hours by addition of 5% trichloroacetic acid (*11*). Results are expressed as mean ± SD in counts per minute of [^{3}H]thymidine incorporated into acid-precipitable material and are from a single experiment representative of three that gave similar results.

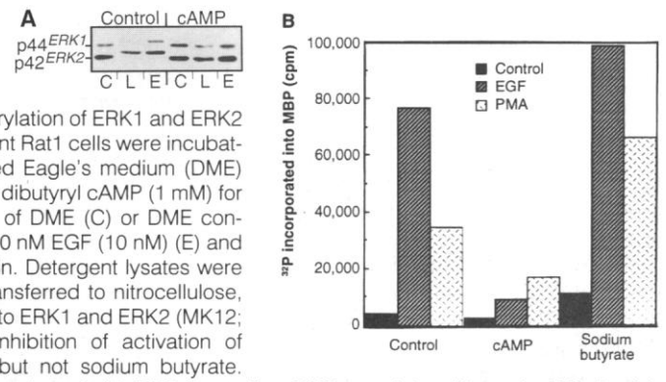

Fig. 1. Effect of dibutyryl cAMP on the activation of ERK1 and ERK2 in Rat1 cells. (**A**) Inhibition of LPA- or EGF-stimulated phosphorylation of ERK1 and ERK2 by dibutyryl cAMP. Quiescent Rat1 cells were incubated with Dulbecco's modified Eagle's medium (DME) (control) or DME containing dibutyryl cAMP (1 mM) for 10 min before the addition of DME (C) or DME containing LPA (10 μM) (L) or 10 nM EGF (10 nM) (E) and incubated for a further 5 min. Detergent lysates were resolved by SDS-PAGE, transferred to nitrocellulose, and blotted with antibodies to ERK1 and ERK2 (MK12; Transduction Labs). (**B**) Inhibition of activation of ERK1 by dibutyryl cAMP but not sodium butyrate. Quiescent Rat1 cells were incubated with DME (control) or DME containing dibutyryl cAMP (1 mM) or sodium butyrate (1 mM) for 10 min before addition of DME (black bars) or DME containing EGF (10 nM, hatched bars) or PMA (100 nM, stippled bars) for a further 5 min. Detergent lysates were immunoprecipitated with E1.2 antiserum, which specifically recognizes ERK1 (*11*), and kinase activity was assayed against MBP in the immune complex. Results are expressed as the amount of ^{32}P incorporated into MBP (counts per minute) and are from a single experiment representative of three that gave similar results.

Raf-1 by growth factors (7). Fractions from Raf-1–transformed cells have MEK kinase activity (9), and Raf-1 activates MEK in vitro (21); thus, Raf is likely to be the link between Ras and the ERK cascade. Stimulation of Rat1 cells with LPA or EGF resulted in the activation of Raf-1, as measured by the phosphorylation of recombinant, catalytically inactive MEK B in immunoprecipitates of antibodies to Raf-1 (anti–Raf-1) (22); irrelevant pre-immune antiserum precipitated no MEK kinase activity (Fig. 4). LPA was at best half as effective at activating Raf-1 as was EGF (Fig. 4), and this correlates with the smaller increase in Ras·GTP activated with LPA compared to that activated with EGF (11). Treatment of Rat1 cells with CT (100 ng/ml) resulted in a complete inhibition of EGF- or LPA-stimulated Raf activation measured in anti-Raf immune complexes (Fig. 4). Thus, cAMP appears to inhibit ERK activation by uncoupling Ras·GTP from the activation of Raf-1.

The effects of cAMP are similar to those of the Rap1a or Krev1 Ras-related GTPase, which can revert Ras transformation when overexpressed (23, 24): Rap inhibits activation of ERKs by either LPA or EGF (11) by inhibiting the coupling of Ras·GTP to Raf (25). Increased concentrations of cAMP result in protein kinase A (PKA)–mediated phosphorylation of Rap1a and Rap GTPase activating protein (24); thus, Rap may itself be a mediator of the effects of cAMP in this system. However, our preliminary results indicate that dibutyryl cAMP does not increase the percentage of Rap in the GTP-bound form in Rat1 cells (12). An alternative and simpler model is that PKA phosphorylates Raf, thereby inhibiting its activation. Raf-1, but not A-Raf or B-Raf, contains a PKA phosphorylation consensus site in the NH_2-terminal regulatory domain, and preliminary experiments have confirmed that PKA is able to phosphorylate recombinant Raf-1 in vitro (12).

Our results are consistent with a model in which cAMP inhibits growth of Rat1 cells by inhibiting Raf activation, although cAMP is also likely to affect cell regulation through other Raf-independent mechanisms (26, 27). Analogs of cAMP inhibit the growth of Ras- and Src-transformed cells (3), which suggests that the targeted use of tissue-specific hormones that increase the intracellular concentration of cAMP may represent a possible avenue of research for therapeutics directed against the Ras pathway.

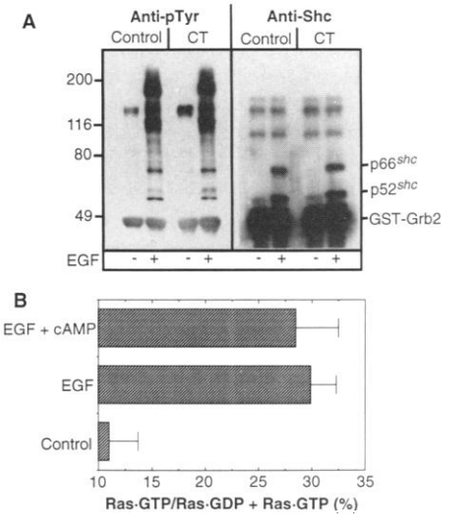

Fig. 3. Signal transduction from the EGFR to Ras is not impaired by cAMP. (**A**) EGFR autophosphorylation and in vitro binding of GST-Grb2 and Shc in Rat1 cells. Quiescent Rat1 cultures were incubated with CT (100 ng ml^{-1} for 1 hour) before stimulation with EGF (10 nM) for 5 min. Duplicate cleared lysates were incubated with GST-Grb2, and bound proteins were resolved by SDS-PAGE, transferred to PVDF membranes, and immunoblotted with either antibodies to phosphotyrosine (anti-pTyr) (PY20 and PY69, left) or antibodies to Shc (right). The positions of prestained molecular size markers (in kilodaltons), the GST-Grb2 fusion protein, and $p52^{shc}$ and $p66^{shc}$ are indicated. (**B**) Lack of effect of cAMP on the EGF-stimulated increases in the percentage of Ras in the GTP-bound state. Elevated cAMP does not impair EGF-stimulated increases in Ras·GTP. Quiescent Rat1 cultures were metabolically labeled with $[^{32}P]PO_4$ for 3 hours and received DME or DME containing 1 mM dibutyryl cAMP for the last 5 min. Cells were then stimulated with EGF, and the amount of Ras in the GTP-bound state was determined as described (11). Results (mean ± SD of duplicates) are from a single experiment representative of three that gave identical results.

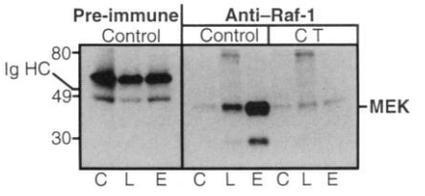

Fig. 4. Cyclic AMP inhibits activation of Raf. Quiescent Rat1 cells were incubated for 1 hour with DME alone (control) or DME containing CT (100 ng/ml) before stimulation with LPA (L) (10 μM) or EGF (E) (10 nM) for 5 min. Proteins from cell lysates were immunoprecipitated with irrelevant antiserum or antiserum to Raf-1 and assayed for MEK kinase activity in the immune complex. Samples were resolved by SDS-PAGE and detected by autoradiography. The positions of catalytically inactive MEK, the immunoglobulin heavy chain (Ig HC), and pre-stained molecular size markers (in kilodaltons) are indicated. Results are from a single experiment representative of three that gave similar results. C, control, no stimulation.

REFERENCES AND NOTES

1. T. W. Rall *et al.*, *J. Biol. Chem.* **224**, 463 (1957); E. W. Sutherland, *Science* **177**, 401 (1972).
2. L. Stryer and H. R. Bourne, *Annu. Rev. Cell Biol.* **2**, 391 (1986); E.-J. Choi, Z. Xia, E. C. Villacres, D. R. Storm, *Curr. Opin. Cell Biol.* **5**, 269 (1993).
3. I. H. Pastan *et al.*, *Annu. Rev. Biochem.* **44**, 491 (1975).
4. A. L. Boynton and J. F. Whitfield, *Adv. Cyclic Nucleotide Res.* **15**, 193 (1983); E. Rozengurt, *Science* **234**, 161 (1986); M. M. Gottesman and R. D. Fleischmann, *Cancer Surv.* **5**, 291 (1986); J. F. Whitfield *et al.*, *Cancer Metastasis Rev.* **5**, 205 (1987); J. E. Dumont *et al.*, *Trends Biochem. Sci.* **14**, 67 (1989).
5. I. Magnaldo *et al.*, *FEBS Lett.* **245**, 65 (1989); C. O. Rock, J. L. Cleveland, S. Jacowski, *Mol. Cell. Biol.* **12**, 2351 (1992).
6. G. Bollag and F. McCormick, *Annu. Rev. Cell Biol.* **7**, 601 (1991); A. Hall, *Curr. Opin. Cell. Biol.* **5**, 265 (1993).
7. S. L. Leevers and C. J. Marshall, *EMBO J.* **11**, 569 (1992); S. M. Thomas *et al.*, *Cell* **68**, 1031 (1992); K. W. Wood *et al.*, *ibid.*, p. 1041; A. M. M. de Vries Smits *et al.*, *Nature* **357**, 602 (1992).
8. C. M. Crews, A. Alessandrini, R. L. Erikson, *Science* **258**, 478 (1992).
9. P. Dent *et al.*, *ibid.* **257**, 1404 (1992); J. M. Kyriakis *et al.*, *Nature* **358**, 417 (1992); L. R. Howe *et al.*, *Cell* **71**, 335 (1992).
10. C. A. Lange-Carter, C. M. Pleiman, A. M. Gardner, K. J. Blumer, G. L. Johnson, *Science* **260**, 315 (1993).
11. S. J. Cook, B. Rubinfeld, I. Albert, F. McCormick, *EMBO J.* **12**, 3475 (1993).
12. S. J. Cook and F. McCormick, unpublished results.
13. Cells were deprived of serum for 36 hours before stimulation with growth factors at 37°C for 5 min. Incubations were terminated by aspiration of the medium and addition of ice-cold lysis buffer [20 mM tris-HCl (pH 8), 1% Triton X-100, 10% glycerol, 137 mM NaCl, 1.5 mM $MgCl_2$, 1 mM EGTA, 50 mM NaF, 1 mM Na_3VO_4, 1 mM phenylmethylsulfonyl fluoride, 20 μM leupeptin, and 10 μg ml aprotinin]. Detergent-insoluble material was removed by centrifugation at 14,000*g* for 10 min at 4°C; protein concentrations were assayed by the Bio-Rad assay and varied by less than 10%. Cell lysates were incubated for 2 hours with E1.2 and E2.1 antisera (11), and protein A–Sepharose beads were added for the last 30 min. Immune complexes were washed three times with lysis buffer and once with kinase buffer [30 mM tris (pH 8), 20 mM $MgCl_2$, and 2 mM $MnCl_2$]. ERK kinase activity was assayed by addition of kinase buffer (30 μl) containing adenosine triphosphate (ATP) (2 μM), MBP (7 μg), and 5 μCi of [γ-^{32}P]ATP and incubation at 30°C for 30 min. Incubations were terminated by addition of hot 4× SDS-PAGE sample buffer (10 μl), and reaction products were resolved by SDS-PAGE (12% gels) followed by autoradiography. The MBP band was excised, and incorporated radioactivity was quantitated by liquid scintillation counting.
14. C. Van Dop *et al.*, *J. Biol. Chem.* **259**, 696 (1984); D. Cassel *et al.*, *Proc. Natl. Acad. Sci. U.S.A.* **74**, 3307 (1977).
15. G. Kaur *et al.*, *Cancer Res.* **52**, 3340 (1992).
16. L. Buday and J. Downward, *Cell* **73**, 611 (1993); M. Rozakis-Adcock, R. Fernley, J. Wade, T. Pawson, D. Bowtell, *Nature* **363**, 83 (1993); N. Li *et al.*, *ibid.*, p. 85; N. W. Gale, S. Kaplan, E. J. Lowenstein, J. Schlessinger, D. Bar-Sagi, *ibid.*, p. 88; S. E. Egan *et al.*, *ibid.*, p. 45.
17. Induction and purification of GST-Grb2 from *Escherichia coli* were as described previously (18). Equal quantities of Rat1 cell lysates were incubated with GST agarose beads followed by incubation with 10 μg of immobilized GST or GST-Grb2 for 2 hours at 4°C. Samples were then washed five times with lysis buffer (inclusion of radioimmunoprecipitation assay buffer washes yielded identical results), drained, and boiled in SDS-PAGE sample buffer. Samples were resolved

by SDS-PAGE (10% gels by Novex) and transferred to poly(vinylidene difluoride) (PVDF) membranes, which were then stained with Coomassie blue to confirm equal sample loading. Filters were then incubated with either antibodies PY20 and PY69 to phosphotyrosine (1:1500 dilution; ICN, Irvine, CA) or polyclonal antibodies to Shc (1:250; Transduction Labs, Lexington, KY). Detection was with horseradish peroxidase–conjugated secondary antibodies and the enhanced chemiluminescence system (ECL, Amersham).
18. E. J. Lowenstein *et al.*, *Cell* **70**, 431 (1992).
19. G. Pelicci *et al.*, *ibid.*, p. 93; J. McGlade, A. Cheng, G. Pelicci, P. G. Pelicci, T. Pawson, *Proc. Natl. Acad. Sci. U.S.A.* **89**, 8869 (1992); M. Rozakis-Adcock *et al.*, *Nature* **360**, 689 (1992).
20. W. Kolch, G. Heidecker, P. Lloyd, U. R. Rapp, *Nature* **349**, 426 (1991); L. Van Aelst, M. Barr, S. Marcus, A. Polverino, M. Wigler, *Proc. Natl. Acad. Sci. U.S.A.* **90**, 6213 (1993); A. B. Vojtek, S. M. Hollenberg, J. A. Cooper, *Cell* **74**, 205 (1993); X.-F. Zhang *et al.*, *Nature* **364**, 308 (1993); P. H. Warne, P. R. Viciana, J. Downward, *ibid.*, p. 352.
21. S. G. Macdonald *et al.*, *Mol. Cell. Biol.*, in press.
22. Proteins from equal quantities of cell lysates from control or stimulated Rat1 cells were immunoprecipitated with 10 μl of Raf-1 polyclonal antiserum [R. Schatzmann, Syntex, Palo Alto, CA] for 2.5 hours, and protein A–Sepharose beads were added for the last 45 min. Immune complexes were washed three times in lysis buffer and once in kinase buffer [30 mM tris (pH 8), 20 mM $MgCl_2$, and 1 mM dithiothreitol] before being resuspended in 30 μl of kinase assay cocktail containing kinase buffer, 0.5 μg of recombinant, baculovirus-expressed catalytically inactive MEK B, 2 μM ATP, and 5 μCi of [γ-^{32}P]ATP per sample. Incubations were for 30 min at 30°C and were terminated by the addition of hot 4× SDS-PAGE sample buffer (10 μl) followed by boiling for 5 min at 95°C. Samples were resolved by SDS-PAGE (10% gels), and gels were stained with Coomassie brilliant blue, dried, and subjected to autoradiography.
23. H. Kitayama *et al.*, *Cell* **56**, 77 (1989).
24. M. Noda, *Biochim. Biophys. Acta* **1155**, 97 (1993).
25. T. Sakoda *et al.*, *Oncogene* **6**, 1705 (1992).
26. J. F. Habener, *Mol. Endocrinol.* **4**, 1087 (1990).
27. F. Lamy *et al.*, *J. Biol. Chem.* **268**, 8398 (1993).
28. We thank T. Evans and G. Bollag (Onyx) for critical reading of the manuscript, T. Palmer (Duke University Medical Center) for advice, S. Macdonald and T. Evans (Onyx) for the recombinant MEK B, and R. Schatzman (Syntex) for antiserum to $p74^{raf\text{-}1}$. S.J.C. and F.M. are supported by a grant from the National Cancer Institute (UO1 CA51992-03) to F.M.

3 August 1993; accepted 13 October 1993

Unidirectional Coupling of Gap Junctions Between Neuroglia

Stephen R. Robinson,* Edith C. G. M. Hampson, Mark N. Munro, David I. Vaney

Gap junctions permit the passage of ions and small molecules between cells, thereby providing a basis for direct intercellular communication. In the rabbit retina, the low molecular weight dyes Lucifer yellow and biocytin passed readily from astrocytes into adjacent astrocytes, oligodendrocytes, and Müller cells. However, the dyes rarely passed from either oligodendrocytes or Müller cells into astrocytes. Unidirectional passage of dye suggests the presence of an asymmetric barrier to the movement of molecules through heterologous gap junctions and indicates the potential for a hierarchy of command between interconnected cells.

Many vertebrate and invertebrate cells are connected by "gap junctions" that provide a route for intercellular communication (*1*). Cellular coupling can be revealed by the intracellular injection of a membrane-impermeant dye of low molecular weight, such as Lucifer yellow (457 daltons) (*2*) or biocytin (373 daltons) (*3*, *4*). The assumption that molecules can pass through gap junctions equally in both directions was challenged by Flagg-Newton and Loewenstein's (*5*) experiments on cocultures of Balb/c and B fibroblasts. They reported that dye injected into B cells diffused readily into neighboring Balb/c cells but that little, if any, dye transferred from injected Balb/c cells into neighboring B cells. This remarkable finding has not been replicated, and its functional significance is unclear because the two cell lines are unlikely to encounter each other outside a petri dish. We now report that asymmetric diffusion of dye occurs between different types of neuroglia (astrocytes, oligodendrocytes, and Müller cells) in the myelinated band of the intact rabbit retina (*6*).

Retinae from adult rabbits were stained with Hoechst 38317 (*7*), and labeled periaxonal astrocytes (*8*) were injected with Lucifer yellow (*9*). We photographed 91 periaxonal astrocytes that had been injected, and in every instance dye had diffused into the majority (>90%) of stained cells within their dendritic fields (mean number of coupled cells, 70; range, 20 to 200; Fig. 1, A and B). Many of these coupled cells (50 to 70%) were neighboring periaxonal astrocytes, whereas the remainder were either oligodendrocytes (Fig. 1, E and F) or astrocytes belonging to other classes. In addition, 58 periaxonal astrocytes were injected with biocytin (*10*). They were coupled to 30 to 300 cells (mean number of coupled cells, 156; Fig. 1G), of which 50 to 70% were periaxonal astrocytes, and the remainder were either oligodendrocytes or astrocytes from other classes.

Some periaxonal astrocytes were also coupled to Müller cells (radial glia): 10 of the 91 injected with Lucifer yellow were coupled to 1 to 12 Müller cells (mean number of coupled cells, 5), whereas 40 of the 58 filled with biocytin were coupled to 1 to 20 Müller cells (mean number of coupled cells, 3). These Müller cells could be found up to 250 μm from the soma of an injected astrocyte. Because the lateral processes of rabbit Müller cells are only about 25 μm long (*11*), such labeling must be due to the diffusion of dye through gap junctions between astrocytes and Müller cells rather than to inadvertent impalement of Müller cell processes. We injected more than 100 Müller cells with Lucifer yellow or biocytin, but they were never coupled to other Müller cells or to astrocytes.

Oligodendrocytes were identified by their characteristic morphology (*12*) (Fig. 1, C, D, F, and H) and by their absence of immunoreactivity to glial fibrillary acidic protein. Approximately half of the stained nuclei at the margin of the myelinated band were oligodendrocytes. Of the 92 oligodendrocytes injected with Lucifer yellow, 90 exhibited no dye diffusion into adjacent cells (Fig. 1, C and D). The remaining 2 oligodendrocytes were surrounded by 8 to 10 lightly labeled oligodendrocytes and Müller cells. Similarly, 49 of the 70 oligodendrocytes injected with biocytin were not coupled. The remaining 21 oligodendrocytes were surrounded by lightly labeled oligodendrocytes and astrocytes (mean number of coupled cells, 49; range, 1 to 150; Fig. 1H).

Our results show that, when periaxonal astrocytes are injected with Lucifer yellow or biocytin, most of the nearby oligodendrocytes and some Müller cells fill with dye. By contrast, when oligodendrocytes are injected, few (if any) of the nearby astrocytes show coupling. Furthermore, when Müller cells are injected, nearby astrocytes are never labeled with dye (Fig. 2).

It is conceivable that the unidirectional spread of dye is attributable simply to damage to the oligodendrocytes (and Müller cells) caused by the injection procedure and consequent closing of their gap junctions. To investigate this possibility, oligodendrocytes were injected with either Lucifer yellow or biocytin, and nearby astrocytes were immediately injected with the other dye (*13*). Of the 23 successful fills, 21 oligodendrocytes were double-labeled. In these 21 cases, dye had passed from astrocytes into oligodendrocytes after the oligodendrocytes

Vision, Touch, and Hearing Research Centre, Department of Physiology and Pharmacology, University of Queensland, Brisbane, Australia 4072.

*To whom correspondence should be addressed.